Effects of Spatial Sampling of Satellite Data on Derived Surface Solar Irradiance

R. T. PINKER AND I. LASZLO

Department of Meteorology, University of Maryland, College Park, Maryland

(Manuscript received 28 March 1990, in final form 4 August 1990)

ABSTRACT

The usefulness of satellites in climate research is primarily due to the ability to produce global, uniformly distributed, long term records of observations. To achieve efficiency in storing, there is a need to compromise on the spatial and temporal resolution of the data. Questions arise about the impact of the reduced resolution on the parameters to be derived. In this study the effect of different spatial sampling of satellite observations on retrieved surface solar irradiance (SW↓) was studied. Our results indicate that sampled (8-km resolution) and areally averaged (50-km resolution) visible brightness is highly correlated; the correlation has a regional, seasonal, and diurnal dependence. Using the two different resolutions of satellite observations, SW↓ was computed for a whole annual cycle. On the average, the results differed by about 8%–9%. Therefore, to validate satellite methods against ground truth to an accuracy which exceeds 8%–9% of the mean, attention should be given to the type of satellite data and ground truth used in the validation process. The scales selected for investigation are of interest to the International Satellite Cloud Climatology Project (ISCCP) B3 sampling.

1. Background

In the last decade, several methods have been developed to estimate surface solar irradiance from satellite observations, as reviewed in Schmetz (1989). Algorithms for estimating surface insolation from satellites utilize either full resolution, spatially sampled, or spatially averaged data. Those who favor the high resolution data argue that such sampling will allow better coupling with ground truth. The spatial averaging is favored because of data compression, and because it was shown that in many situations (e.g., drifting clouds) SW↓ estimates from areally averaged instantaneous satellite observations may be more appropriate for coupling with time-averaged surface measurements (Tarpley 1979). In the validation process, it is difficult to discern errors due to algorithm, satellite sampling, or incompatibility between the temporal scales of the satellite and the ground observations. Based on independent estimates by various investigators, it is believed that monthly means of surface insolation can be determined to within ± 10 W m^{-2} (WCP-115 1986). These estimates do not consider the effects of satellite sampling on the inferred surface irradiance.

Under the International Satellite Cloud Climatology Project (ISCCP), the collection of a uniform global climatology of sampled satellite measured radiances from an international network of operational weather satellites in the visible and thermal IR was initiated. There are five geostationary satellites: GOES-E and GOES-W (U.S.); Meteosat (European community); GMS (Japan); Insat (India); and at least one polar orbiting satellite (Schiffer and Rossow 1985). Each geostationary satellite has imaging times of approximately half an hour and can scan about one third of the globe; the polar orbiting satellites observe the globe twice a day. While many of the operational satellites can observe the earth at high spatial and/or temporal resolution, due to limited storage capacity of the satellite recording systems, only sampled data are stored.

It is anticipated that the data obtained under ISCCP would be a primary source of information for the study of cloud radiative feedbacks in climate and for the improvement of climate models; the Joint Scientific Committee (JSC)/World Climate Research Program (WCRP) Working Group on Radiative Fluxes (WCRP-10 1988) concluded that such data would be also useful for deriving surface irradiance and for validating surface insolation algorithms (Whitlock et al. 1990). The question therefore arises: what is the affect of the sampling used on the derived surface solar irradiance?

The relationship between satellite measured radiance and surface irradiance is not necessarily linear. The surface irradiance over a 50×50 km region, obtained by averaging the estimates from the full resolution pixels is not necessarily the same as the insolation derived from the spatial average of the top of the atmosphere (TOA) radiance over the same region. Yet, over certain spatial scales, the relationship was found to be quasi-linear (Gautier et al. 1984). Similarly, a single sampled radiance may not be representative of the average con-

Corresponding author address: Dr. Rachel T. Pinker, Department of Meteorology, University of Maryland at College, 2213 Computer and Space Science Building, College Park, MD 20742-2425.

ditions of a larger region. Therefore, the effect of sampling on the inferred irradiance is of concern.

In the present study, a unique experimental dataset of GOES-East (E) observations covering a whole annual cycle is used to study the difference in surface insolation as computed from 8-km and 50-km averaged pixels (see section 4b). The ISCCP B3 data are 8-km pixels sampled about every 30 km; it is of interest for the ISCCP B3 sampling to determine how well the 8-km pixel represents a 50-km area. The data used in this study and a brief description of the ISCCP B3 data will be discussed in section 2. An analysis of the temporal variability in satellite brightness observations at selected locations will be presented in section 3, and the effects of the satellite spatial resolution on the derived surface radiative fluxes over a whole annual cycle will be discussed in section 4. A review of what is presently known on the spatial variability of ground insolation will be presented in section 5. Validation experiments will be given in section 6, and a summary will be given in section 7.

2. Data used

a. GOES data

The developmental satellite dataset contains 8 km resolution Visible and Infrared Spin Scan Radiometer (VISSR) pixels from the GOES-East (E) in the visible region (0.55–0.75 μm). The satellite data were provided by NOAA/NESDIS (J. D. Tarpley, private communication). Eleven visible observations and five IR observations are collected each day for each site. The data are in the form of counts that are dimensionless quantities proportional to the square root of the intensity in the associated spectral region. The average visible count of 5 × 5 array of pixels and the center pixel count of the array were collected (Fig. 1). Each 5 × 5 array of pixels covers an area on the surface of about 50 km on each side. The standard deviation of the visible count of each individual pixel from the average count of the 5 × 5 array of pixels is also computed and stored for each observation.

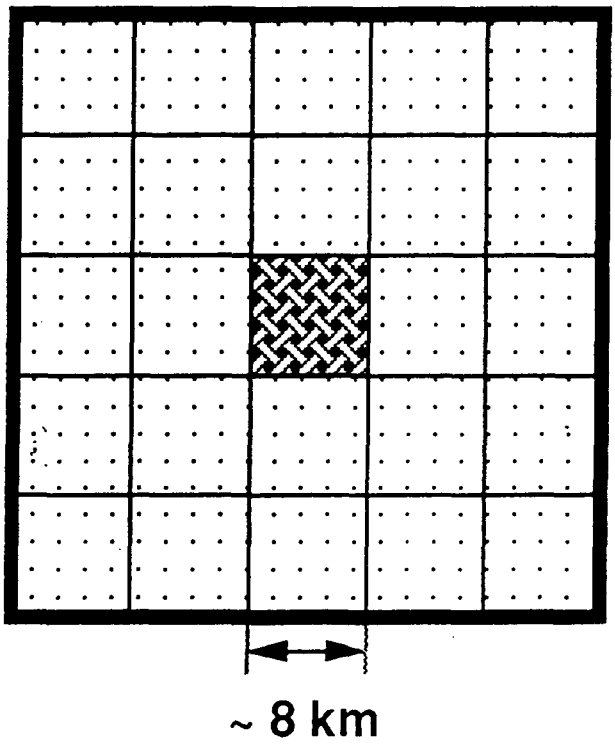

FIG. 1. The sampling scheme of the training dataset provided by NOAA/NESDIS.

b. ISCCP B3 data

The spatial resolution of the raw images of the ISCCP data ranges between 1–2 km in the visible and 4–12 km in the infrared (IR). The Global Processing Center (GPC) at NASA/Goddard Institute for Space Studies (GISS) produces the primary global-radiance-data product B3, which has a nominal spatial resolution of 8 km, sampled approximately every 30 km; time resolution of 3 hours (Schiffer and Rossow 1985); and the navigation is within one B3 pixel. There is legitimate concern about the compatibility of a radiance averaged over an 8-km pixel and one averaged over a 50-km pixel.

3. Temporal variability in satellite brightness observations at several locations

GOES-E satellite data of the type described in section 2a were available to us for about one hundred different locations in North and South America, for periods of several months to several years. In this study locations were selected for which information was available for at least one annual cycle. They represent different surface types; e.g., desert (White Sands, NM), agricultural land (Delmarva Peninsula, MD), and ocean (Table 1). White Sands is frequently used as a calibration site for the VISSR instrument on the GOES satellites (Wark et al. 1980; Hovis et al. 1985; Frouin and Gautier 1987). The Delmarva Peninsula is frequently used in validation experiments by East Coast scientists (Kaufman et al. 1986). Ocean sites were added to facilitate comparison with land surfaces of lower spatial coherence than water (Coakley and Bretherton 1982). To study the relationship between the center pixel visible count and the mean visible count of the 5 × 5 array of pixels, the data were subdivided into three time intervals. M-morning (8–11 a.m.); N-noon (11–2 p.m.); and A-afternoon (2–4 p.m.), for two months at a time. For each subset, bivariate scatter plots were generated between the target average and center pixel count normalized to the solar zenith angle (Figs. 2a–b). An ex-

TABLE 1. Coordinates of locations used in study of spatial variability in satellite brightness observations.

	Coordinates of points	
	Latitude	Longitude
White Sands, NM	32.80	−106.20
	32.81	−106.25
	32.81	−106.34
	32.88	−106.25
	32.88	−106.34
	32.96	−106.25
	32.96	−106.34
Delmarva, MD	38.98	−77.47
Ocean	−.82	−89.54
	25.90	−89.70
	34.90	−72.90
	43.93	−60.01
	47.50	−87.00

ample of the available statistics is given in Table 2 for the first two-month period (January–February); each of the three locations; each of the three daytime intervals, M, N, and A; and all time intervals merged (3). The number of cases (N), the correlation coefficient (R), the regression constants, the Residual Mean Square Error (RMSE), the mean and standard deviations of the target average counts (X), and the center count (Y) are also specified.

The seasonal variation of the correlation coefficients, R, for each location; each daytime interval M, N, and A; and all three cases combined (3) is presented in Figs. 3a–c. As evident, the correlation coefficient exhibits a distinct diurnal and seasonal variation. For instance, over White Sands (Fig. 3a), the correlation coefficient, R, is low (0.7) during the morning hours of May–June (M–J) and is high (0.97) between September and December. Over the Delmarva peninsula, the correlation is lowest during the afternoon (0.92) of July–August (J–A). Over the ocean there seems to be a minimum between July–September, for all the daytime intervals.

The correlation patterns can be interpreted in terms of the climatologies of these regions. For instance, the climate of the White Sands area is characterized by frequent changes in air mass and by a nocturnal maximum of thunderstorm activity. These storms, possibly associated with a "low-level jet" (Bonner 1966), occur between 12 and 8 a.m. LST. The cloud bands associated with these storms persist well into the morning hours. This would suggest the possibility of a decrease in correlation between the different sampling scales during the morning hours. The Washington, D.C. area averages thirty thundershowers per year with seventy-five to eighty percent of these occurring between May and August (Moyer 1968); twenty-five percent of the annual total number occurs in the afternoons of July. Decrease of correlation between the center and mean counts in the afternoon during the summer months is a result of the relatively small size of the convective clouds.

Because of the regional, seasonal, and diurnal variation in the correlation between the sampled and mean

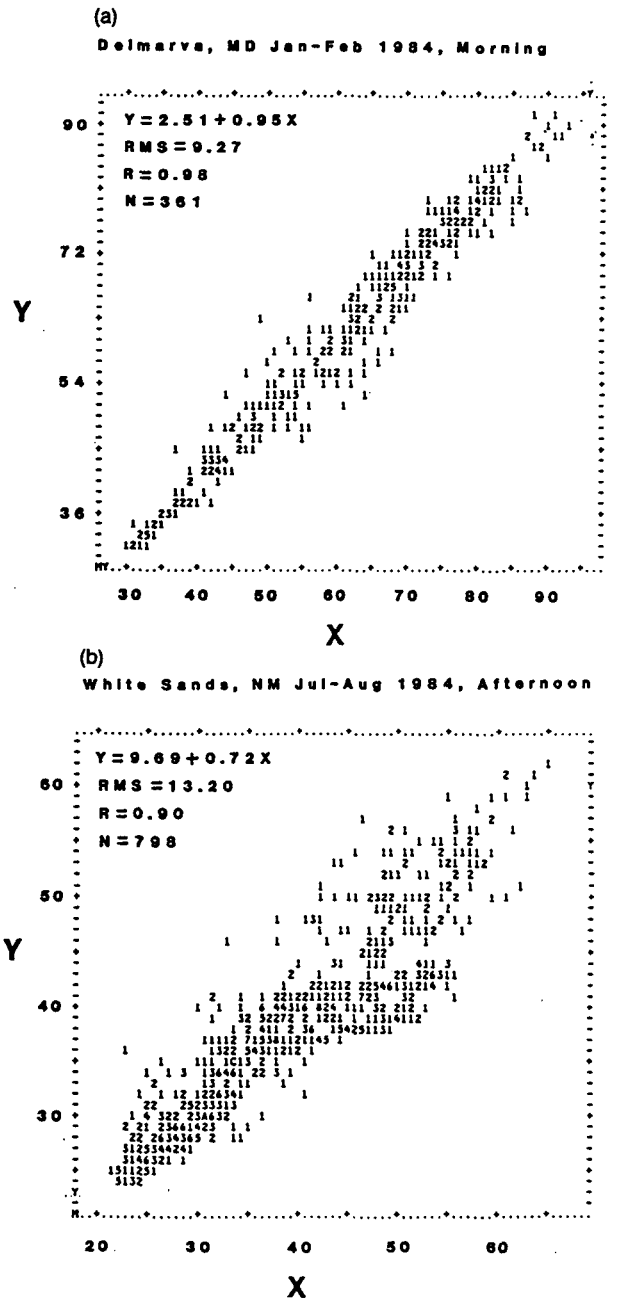

FIG. 2. Scatter diagram between the target average count, X, (50-km pixel) and center count, Y, (8-km pixel) for: (a) Delmarva, MD, January–February 1984 [morning (M) data only]; $\bar{X} = 61.8$; $\bar{Y} = 61.4$; $\sigma_x = 15.5$; $\sigma_y = 15.1$. (b) White sands, NM, July–August 1984 [afternoon (A) data only]; $\bar{X} = 39.2$; $\bar{Y} = 38.0$; $\sigma_x = 10.2$; $\sigma_y = 8.2$. The counts were normalized by the cosine of the solar zenith angle. The numbers in the scatter diagrams denote the number of cases at each location. A = 10 cases; B = 11 cases; C = 12 cases.

TABLE 2. Selected statistics derived between the target average (X) and center (Y) brightness.[a] The data were segregated into intervals of 2 months (e.g., January–February); for each day, there are three intervals: M-morning (8–11); N-noon (11–2); A-afternoon (2–4). Statistics were derived for all three cases merged (Time: 3). N-number of cases; R-correlation coefficient; RMSE-residual mean square error.

					Reg. coeffs.			Mean		Std. dev.	
Location	Month	Time	N	R	a	b	RMSE$_y$	X	Y	X	Y
Delmarva	J/F	M	57	.969	2.16	.966	13.56	66.3	66.1	14.9	14.9
Delmarva	J/F	N	169	.979	2.07	.959	8.44	59.3	59.0	14.4	14.1
Delmarva	J/F	A	135	.983	3.30	.941	8.64	62.9	62.5	16.7	15.9
Delmarva	J/F	3	361	.980	2.51	.954	9.87	61.8	64.4	15.5	15.1
White Sands	J/F	M	791	.864	18.06	.650	13.86	70.6	63.8	9.8	7.4
White Sands	J/F	N	1162	.724	22.70	.467	11.63	54.4	48.1	7.7	4.9
White Sands	J/F	A	642	.849	13.48	.642	20.91	60.5	52.3	11.4	8.6
White Sands	J/F	3	2595	.883	9.76	.726	20.19	60.8	53.9	11.7	9.6
Ocean	J/F	M	388	.976	2.71	.948	26.94	48.1	48.3	24.8	24.0
Ocean	J/F	N	824	.975	2.07	.956	23.57	49.3	49.3	22.4	22.0
Ocean	J/F	A	522	.977	1.98	.957	25.30	52.9	52.6	24.3	23.8
Ocean	J/F	3	1734	.946	2.22	.954	24.80	50.1	50.0	23.6	23.0

[a] $y = a + bX$

fields, the impact of sampling on derived radiative parameters has to be evaluated over a whole annual cycle for different climatic regions. In what follows, we estimate the differences in the derived surface solar irradiance caused by sampling for a whole annual cycle for continental and oceanic sites.

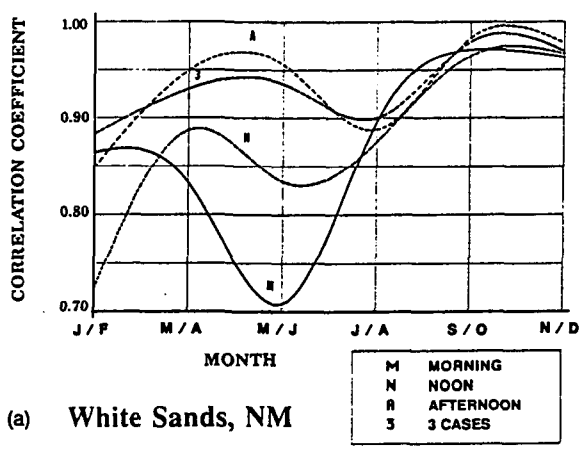

(a) White Sands, NM

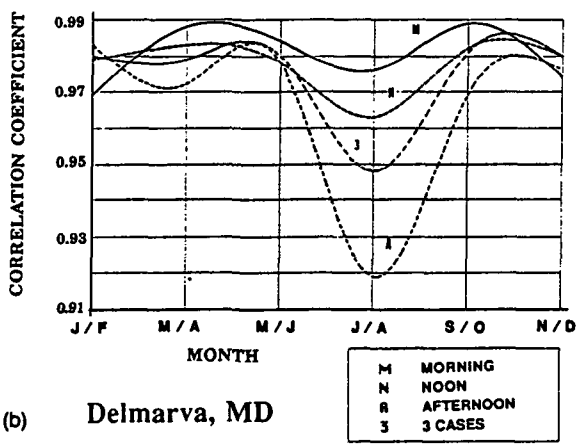

(b) Delmarva, MD

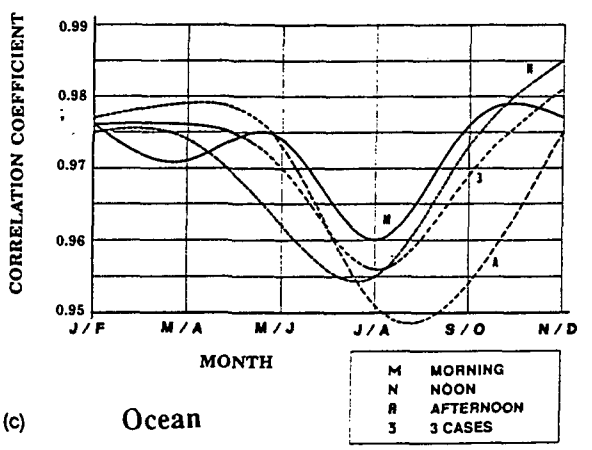

(c) Ocean

FIG. 3. The annual variation of the correlation coefficients between the target (50 km) and center (8 km) visible counts, (normalized by the cosine of the solar zenith angle) for: morning (M); noon (N); afternoon (A); and all three daytime periods combined (3). Location: (a) White Sands, NM; (b) Delmarva, MD; (c) oceanic locations.

4. Effects of satellite spatial sampling on the inferred surface irradiance

a. Model used

The spectral model of Pinker and Laszlo (1990) for deriving surface insolation from satellite observations has been used to assess the effects of satellite sampling on the inferred insolation. The solar spectrum from 0.2 to 0.7 μm is split into 4 equally spaced intervals in the model; the region from 0.7 to 4 μm is represented by a single interval. Parameterization is applied to the optical properties of Rayleigh scattering, water vapor absorption, aerosol absorption and scattering, cloud absorption and scattering, and ozone absorption. Specifically:

- The parameterization of shortwave radiative properties of clouds as given in Stephens et al. (1984) is used.
- The land–albedo models of Briegleb et al. (1986) are adopted to prescribe the surface reflectance as a function of solar zenith angle and wavelength.
- Four atmospheric aerosol profiles (MAR-I, MAR-II, CONT-I, and CONT-II) of the Standard Radiation Atmosphere (SRA) (WCP-55 1983) and the five standard atmospheres [tropical; midlatitude (summer and winter); and subarctic (summer and winter) (Kneizys et al. 1980)] have been implemented in the solar model. For each layer, the aerosol models give the extinction coefficients, single scattering albedos, and asymmetry parameters as functions of wavelength and aerosol type (continental; maritime; background stratospheric; and upper atmospheric).
- The standard atmospheres are used to specify the ozone and water vapor amounts. The Lacis and Hansen (1974) parameterization of water vapor absorption is used for computing the effective water vapor amount in each atmospheric layer. The number of layers of the solar model is determined according to the aerosol model selected (five or six).

Estimation of the shortwave radiation at the surface (SW↓) is obtained in two steps. First, pairs of planetary albedos and SW↓ are calculated using the delta-Eddington approximation of radiative transfer in the shortwave spectrum. The calculations are performed for clear and cloudy sky separately, with various values of aerosols and cloud optical depths. The calculations are repeated for several values of solar zenith angle and various surface models. In the second step, planetary albedos are derived from satellite counts, using current calibration of the sensor, clear–cloudy discrimination, and narrow-to-broadband transformations. The satellite derived planetary albedos are matched with those obtained in the first step and used to get an estimate of the surface insolation.

b. Results

In what follows we estimate differences in the surface solar irradiance due to satellite sampling used. Specifically, the following surface solar irradiances were computed:

$F(\bar{X})$ – using the mean value ($\bar{X}$) of the target average count;

$F(\bar{Y})$ – using the mean value ($\bar{Y}$) of the center count;

$F(\bar{X}+)$ – using $\bar{X}$ + RMSE$_x$;

$F(\bar{X}-)$ – using $\bar{X}$ − RMSE$_x$;

$F(\bar{Y}+)$ – using $\bar{Y}$ + RMSE$_y$; and

$F(\bar{Y}-)$ – using $\bar{Y}$ − RMSE$_y$.

Estimates of surface solar irradiance were obtained for Delmarva, MD, and for the oceanic locations of Table 1 for six two-month intervals as presented in Table 3. For Delmarva, the Type 2B spectral albedo model of Briegleb et al. (1986) was used. This spectrally integrated albedo was then scaled to agree with the seasonal values as documented in Matthews (1983). The albedo of ocean was assumed to be constant (6%). Since the majority of the sites in Table 1 are at midlatitudes, the midlatitude summer and winter profiles of the standard atmospheres (Kneizys et al. 1980) were used throughout the year. For Delmarva, MD, the CONT-I aerosol profile was used; for the oceanic locations the MAR-I aerosol profile was used (WCP-55 1983).

As evident from Table 3, the computed surface solar fluxes $F(\bar{X})$ and $F(\bar{Y})$ are similar, however, the absolute values of $\Delta F(\bar{X}+)$; $\Delta F(\bar{Y}+)$ and $\Delta F(\bar{X}-)$; and $\Delta F(\bar{Y}-)$ are different. This is because the surface solar flux is not a linear function of the atmospheric optical depth (Pinker and Ewing 1985). The decrease and increase of the mean values ($\bar{X}$) and ($\bar{Y}$) lead to flux estimates that are not symmetric. In few cases one can find negative values, indicating a drop in the surface flux (Table 3). This can be explained to be a result of the clear–cloudy discrimination scheme used in the model; namely, predetermined values of planetary albedos are used as criteria to distinguish between clear and cloudy situations. Planetary albedos, initially corresponding to a cloudy situation after being reduced by the RMSE, can fall into the clear category with a relatively high aerosol optical thickness. In contrast to clouds, aerosols have strong absorption in the visible; the surface solar flux associated with heavy aerosol content is lower than the solar flux associated with a cloud of same optical depth.

The percentage change in the computed SW↓ as a result of adding (subtracting) the RMSE$_x$ to (from)

TABLE 3. The satellite derived mean surface solar flux (W m^{-2}) $-F(X)$ and $-F(Y)$ for Delmarva, MD, and the ocean sites. $\bar{X}$ is the mean value of the target average counts; $\bar{Y}$ is the mean value of the central counts. The change in the surface flux obtained by adding and subtracting the RMSE to the mean values were also computed. The following notations apply:

$$\Delta F(\bar{Y}+) = F(\bar{Y}) - F(\bar{Y} + \mathrm{RMSE}_y)$$

$$\Delta F(\bar{Y}-) = F(\bar{Y}) - F(\bar{Y} - \mathrm{RMSE}_y)$$

$$\Delta F(\bar{X}+) = F(\bar{X}) - F(\bar{X} + \mathrm{RMSE}_x)$$

$$\Delta F(\bar{X}-) = F(\bar{X}) - F(\bar{X} - \mathrm{RMSE}_x)$$

RMSE_x and RMSE_y are the RMSE from the target count–central count regression and from the central count–mean count regression, respectively.

			Flux (W m^{-2})					
Location	Month	Time	$F(\bar{X})$	$F(\bar{Y})$	$\Delta F(\bar{Y}+)$	$\Delta F(\bar{Y}-)$	$\Delta F(\bar{X}+)$	$\Delta F(\bar{Y}-)$
Delmarva	J/F	1	291.4	292.2	−21.8	23.8	−21.7	23.9
	J/F	2	367.5	370.9	−28.3	29.0	−29.1	29.0
	J/F	3	288.9	290.7	−12.2	7.7	−12.9	9.5
	J/F	4	343.6	347.2	−32.5	30.2	−33.7	31.2
	M/A	1	479.2	475.0	−37.5	35.8	−37.6	35.9
	M/A	2	528.0	526.7	−49.1	54.9	−51.0	56.8
	M/A	3	439.7	444.1	−43.9	41.5	−46.3	43.7
	M/A	4	485.9	487.7	−59.0	61.1	−61.4	63.4
	M/J	1	660.2	667.1	−47.8	1.1	−50.2	8.0
	M/J	2	750.1	753.6	−65.2	73.4	−68.4	77.0
	M/J	3	580.5	583.9	−54.8	50.5	−57.4	52.8
	M/J	4	681.7	687.1	−76.8	71.3	−80.3	74.5
	J/A	1	690.9	685.6	−49.2	−37.1	−50.6	−31.6
	J/A	2	762.3	773.3	−66.5	32.4	−72.3	43.4
	J/A	3	601.4	618.3	−59.8	−17.3	−73.0	−11.5
	J/A	4	706.1	721.6	−85.6	81.8	−97.3	91.0
	S/O	1	423.3	427.3	−33.9	32.3	−35.5	33.8
	S/O	2	610.5	609.3	−43.1	4.8	−45.3	3.7
	S/O	3	412.8	418.0	−34.2	33.7	−36.7	36.2
	S/O	4	514.5	519.2	−58.6	55.1	−62.2	58.2
	N/D	1	307.9	304.4	4.3	24.4	0.8	25.1
	N/D	2	441.1	442.1	−23.7	42.4	−25.3	−40.6
	N/D	3	236.2	233.6	3.2	15.8	0.6	15.7
	N/D	4	402.3	400.6	−28.6	28.3	−29.6	29.3
Ocean	J/F	1	421.6	420.4	−33.2	29.9	−34.2	30.6
	J/F	2	479.7	480.6	−59.2	53.7	−60.5	54.8
	J/F	3	353.5	354.9	−24.1	20.3	−24.7	21.7
	J/F	4	472.7	473.7	−63.4	57.2	−61.8	58.6
	M/A	1	596.9	605.8	−51.3	47.5	−54.6	49.7
	M/A	2	720.0	727.2	−64.8	58.8	−68.5	62.0
	M/A	3	509.4	512.8	−42.3	39.1	−44.0	40.5
	M/A	4	662.8	671.9	−77.8	70.3	−81.8	73.6
	M/J	1	721.6	723.2	−53.3	48.8	−55.2	50.3
	M/J	2	887.9	893.9	−67.2	68.1	−71.3	71.6
	M/J	3	686.9	689.9	−43.7	42.5	−46.4	44.8
	M/J	4	842.0	846.9	−73.0	67.3	−76.8	70.6
	J/A	1	686.1	683.6	−63.5	56.2	−67.4	59.5
	J/A	2	843.3	848.1	−70.0	63.9	−76.6	69.5
	J/A	3	643.8	646.3	−53.3	50.1	−57.5	53.5
	J/A	4	794.0	796.6	−84.5	77.2	−91.0	82.4
	S/O	1	523.3	525.2	−45.6	42.1	−48.2	44.3
	S/O	2	691.6	692.2	−54.5	48.7	−57.2	51.1
	S/O	3	477.6	478.5	−47.9	42.8	−49.4	44.9
	S/O	4	626.8	628.6	−76.9	68.8	−80.9	72.1
	N/D	1	393.4	393.4	−18.4	0.0	−19.6	0.0
	N/D	2	481.8	482.8	−37.9	35.0	−37.9	35.7
	N/D	3	313.7	313.6	0.0	32.5	0.0	32.6
	N/D	4	484.5	485.8	−43.0	40.1	−44.3	41.3

the mean target count, ($\bar{X}$), and RMSE$_y$ to (from) the mean central count, ($\bar{Y}$), were computed (Fig. 4). For all cases considered, the mean and median values of the resulting changes in SW↓ are between 8%–9%. This would indicate that were we to use the central pixel brightness instead of the mean target brightness, or vice versa, the mean (or median) RMSE in the inferred surface solar irradiance would be between 8%–9%. Therefore, to validate satellite methods for deriving surface irradiance to a higher accuracy, the validation sampling has to be designed accordingly.

5. Spatial variability in surface SW↓

We have discussed the effects of satellite sampling on derived surface solar irradiance. It was shown that had we used the center pixel instead of the mean target brightness, or vice versa, the mean (or median) RMSE

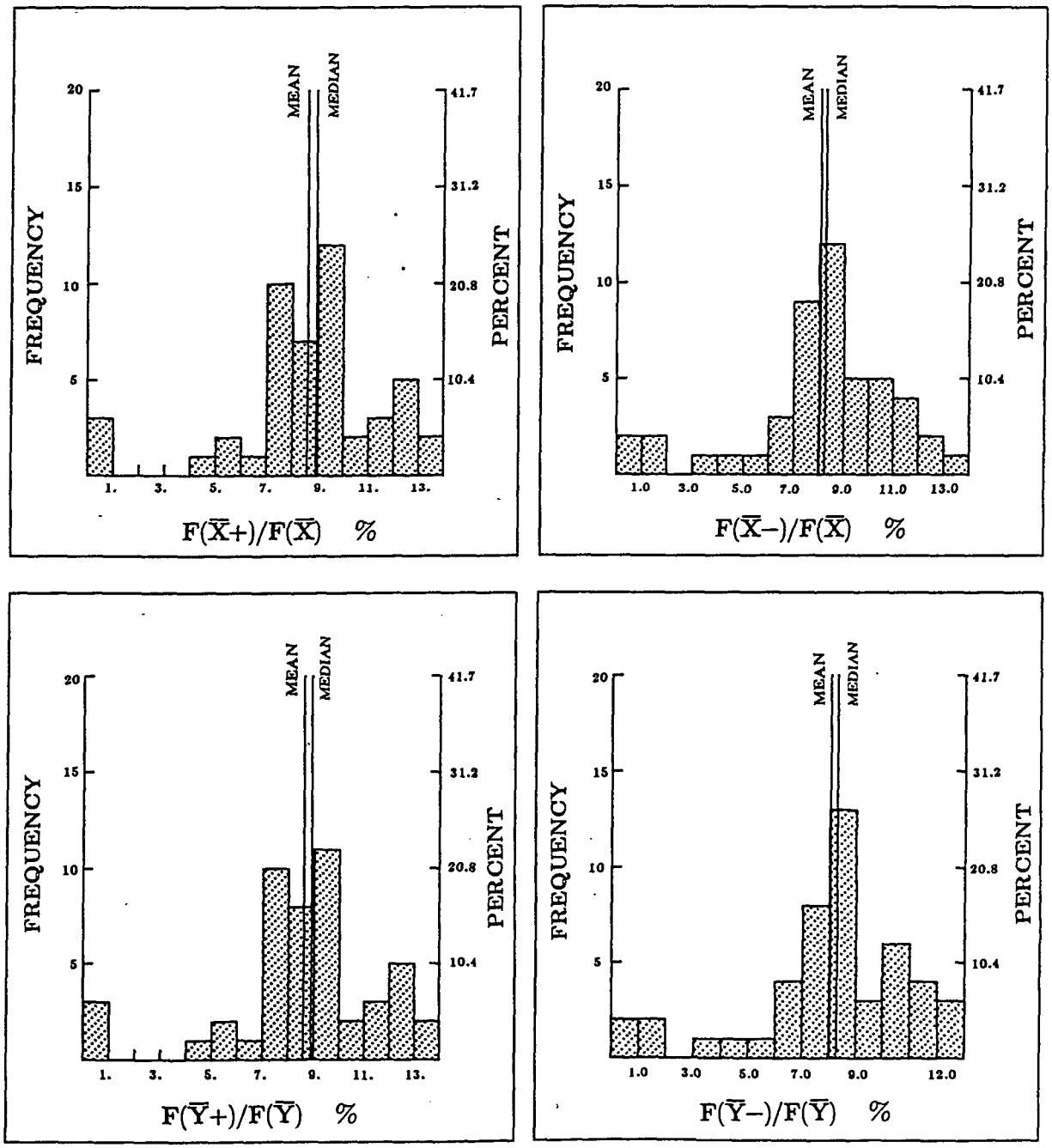

FIG. 4. The frequency distributions of the percentage change in the computed SW↓ as a result of adding and subtracting the RMSE$_x$ and RMSE$_y$ to $\bar{X}$ and $\bar{Y}$ respectively.

in the inferred SW↓ would be between 8%–9%. In order to assess which sampling gives better estimates of the true insolation received at the ground, we first have to establish the requirements on surface sampling necessary to resolve this question. We will briefly review what is known on the spatial variability of surface SW↓.

Early attempts to determine an acceptable distance between SW↓ measurement stations, given an acceptable interpolation error, were summarized by Gandin (1970). More recent attempts to address such issues (e.g., Wilson and Petzold 1972; Suckling and Hay 1976; Hay and Suckling 1979; Dugas and Heuer 1985) involve the calculation of the mean and standard deviation of daily differences in incoming SW↓ between station pairs, and plotting it as a function of the distance between the stations. Some investigators use coefficient of variability, C_v, i.e., the standard deviation divided by the mean solar irradiance.

In Fig. 5, the standard deviations of one-day averaged differences of SW↓ from a mean as a function of station distance are illustrated. They were obtained by: (A) Atwater and Ball (1978); (B) Suckling and Hay (1976); (C) Granger (1980); (D) Wilson and Petzold (1972); (E) present study (to be described in the Appendix). If curves A; B; C; D; E (Fig. 5) were to be extrapolated to a distance of 50-km station separation, the standard deviations would range between 1.5–2.5 MJ m^{-2} day^{-1}. If we assume an average summer isolation of 30 MJ m^{-2} day^{-1}, then an average standard deviation of 2 MJ m^{-2} day^{-1} would be about 7% of the mean value. The operational accuracy of instruments measuring SW↓ is estimated to be ±5% under the best circumstances (Latimer 1980). Assuming an average accuracy of 7%, the error in the station difference values can be $\sqrt{(7\%)^2 + (7\%)^2} \sim 10\%$, which is above the estimated error due to station separation distance.

In a recent study, Burt (1985) presents an analysis of the relationship between network density and interpolation. He claims that error measures used previously (e.g., coefficient of variability, C_v) are likely to overstate expected errors for short time periods. His empirical analysis suggests that when distances of a few hundred kilometers are considered, root-mean-square interpolation errors in daily solar irradiance are significantly smaller than results based on C_v would indicate. There is very little information on the spatial variability for scales less than 100 km. Aguado (1986) did study local-scale variability of daily SW↓ in San Diego County, California. He claims that unlike the results of previous studies at larger regional scales, no mathematical function could be obtained relating the magnitude of the coefficient C_v to between-station distance for separations ranging from 9 to 62 km. This seems to be consistent with the 60-km "zone of indif-

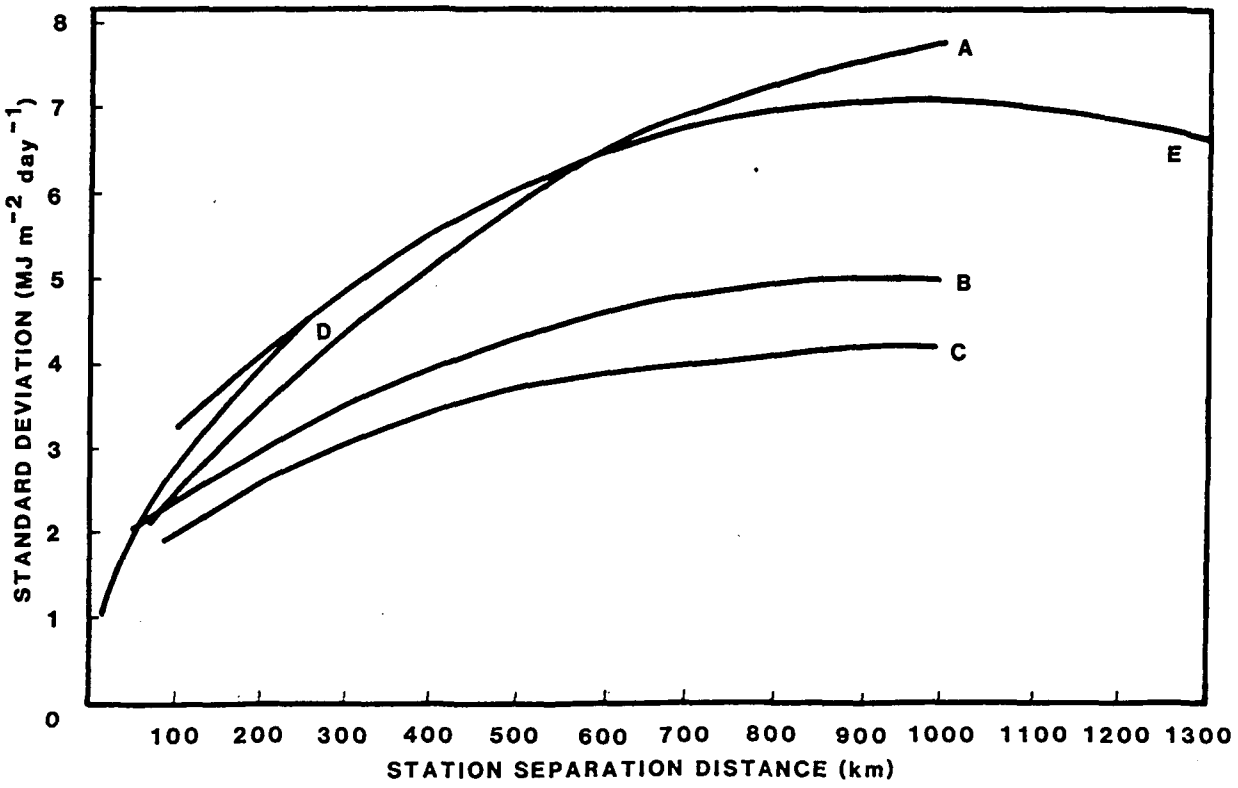

FIG. 5. Standard deviations of one-day averaged differences of SW↓ from a mean, as a function of station separation distance, obtained by: (A) Atwater and Ball (1978); (B) Suckling and Hay (1976); (C) Granger (1980); (D) Wilson and Petzold (1972); (E) present study.

ference" reported on by Baker and Skaggs (1984) using sunshine data. The above arguments would justify the use of one ground observing station for the verification of an algorithm, which uses as input satellite data that are sampled or averaged over 50-km pixels or less.

6. Validation experiments

For validating the SW↓ estimates obtained from the different satellite samplings, two locations were selected (Toronto, Canada, 43°48'N, 79°33'W; and Elora, Canada, 43°30'W; 80°24'W) where SW↓ and colocated satellite data (of the type described in section 2a) were available. The surface observations were provided by the Canadian Climate Center of the Atmospheric Environmental Service, as documented in Phillips and Aston (1980).

Daily totals of solar irradiance were computed for July 1984 using the center count and the mean target count. The ozone amount (0.318 atm–cm) and the vertical profiles of pressure, temperature, and water vapor were assumed to correspond to those of the mid-latitude summer atmosphere (Kneizys et al. 1980). The CONT-I profile of the Standard Radiation Atmospheres (WCP-55 1983) was used to describe the vertical distribution of aerosols. It consisted of continental aerosols in the planetary boundary layer, tropospheric aerosols up to 12 km, background stratospheric aerosols up to 30 km, and upper atmospheric aerosols above 30 km. The average optical depth of these layers at 0.55 μm were 0.2, 0.025, 0.005, and 0.00012 respectively. The surface types corresponding to the geographical coordinates of the two stations were identified using the one degree resolution atlas of vegetation and seasonal albedo data of Matthews (1983) (i.e., deciduous forest with evergreens, Type 10 of Matthews). This information coupled with the spectral and angular albedo models of Briegleb et al. (1986) was used to prescribe the surface reflectance as a function of the solar zenith angle and wavelength. In these models, each surface type is considered to consist of two components. For Type 10 of Matthews (Type 4 of Briegleb et al. 1986) the surface is composed of 50% deciduous forest and 50% evergreen forest. The broadband albedo computed from the model for solar zenith angle of 60 degrees with the above parameters is 0.15. Matthews' compilation of the seasonal albedos gives a higher value (0.18) for July. Iqbal (1983, p. 292) reported 0.25 for the July albedo of Toronto. Therefore, we scaled the directional surface albedos of Briegleb et al. to give the higher value (0.18) as a daily average surface albedo.

The results of satellite-derived surface solar irradiance and ground observations are presented in Fig. 6 for Elora. As evident, estimates derived from the target average counts are in better agreement with ground measurements. For Toronto, the use of the center count seemed to be in better agreement with the observations for part of the observing period. It is quite possible that for certain cloud conditions, one type of satellite sampling would result in SW↓ estimates that are in better agreement with observed values; for other cloud conditions, different satellite sampling could be more appropriate for coupling with ground observations.

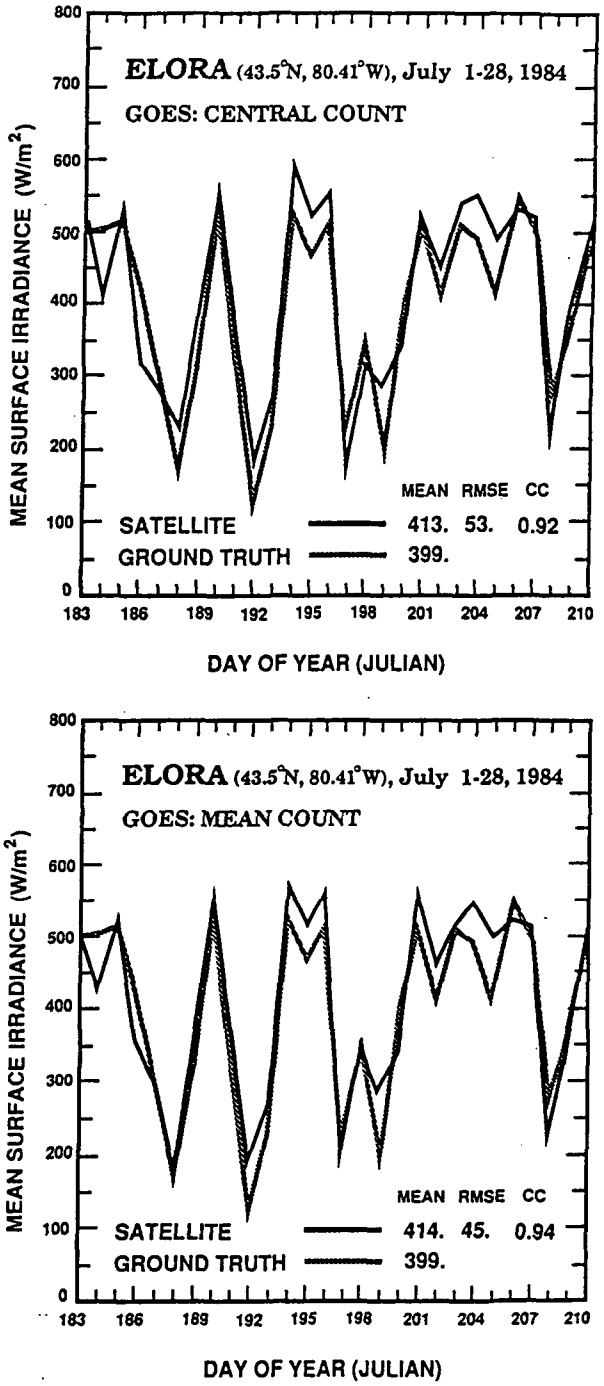

FIG. 6. Time series of satellite derived (solid line) and ground observed (dashed line) surface solar irradiance at Elora, Canada, using "central" and "target average" counts. (a) Elora, central count; (b) Elora, target count. Relevant statistics [mean, RMSE, and correlation coefficient (CC)] are also given.

Therefore, comparisons over a whole annual cycle for different climatic conditions should be made before a conclusion can be reached on the performance of an algorithm. Possibly the *point* validation concept should be abandoned in favor of a *regional* validation approach where the areally averaged computed values are compared against areally averaged ground observations. As illustrated in Fig. 7, the spatial distribution of eight day averaged surface irradiance (W m^{-2}) over part of Texas, derived from GOES-E visible 8-km and 50-km averaged counts, is very similar. Possibly one could compute the areally averaged surface irradiance as derived from the differently sampled satellite data and compare it with an areally average as observed by a ground observing network whose separation is not to exceed 50 km. This procedure could not be followed in the present study because the ground observing stations (numbered from 1 to 7) were not evenly distributed.

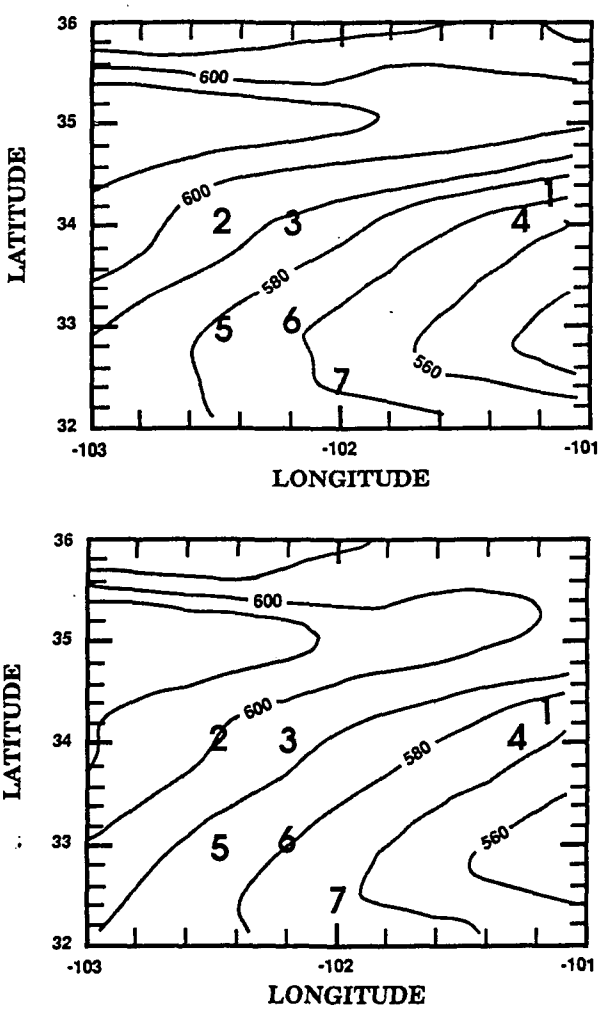

FIG. 7. The spatial distribution of eight-day average surface irradiance (W m^{-2}) over part of Texas, derived from GOES-E visible counts, using: (a) central counts; (b) mean target counts. The numbers from 1 to 7 represent the location of stations where ground truth was available. The eight-day average measured irradiance (W m^2) for each of the seven locations was: 603; 608; 592; 590; 524; 591; and 517 W m^2, respectively.

7. Summary

The development of techniques to derive Surface Radiation Budget (SRB) from satellite observations is one of the goals of the World Climate Research Program (WCRP). The SRB plays an important role in all the new climate research initiatives; e.g., TOGA (WCP-92 1984); WOCE (WCRP-21 1989); ISLSCP (ESA SP-248 1986); and GEWEX (WCRP-5 1988). Before these methods can be used with confidence, there is a need to validate them. Due to inherent limitations, the process of validation in itself is difficult (e.g., the spatial and temporal incompatibility of the satellite and ground observations; the satellite data are sampled rather than areally averaged). In principle, the latter limitation could be removed by generating high resolution validation datasets. However, questions will still remain regarding the errors in the inferred surface fields when using routinely sampled data. In the present study we attempted to address some of the above issues.

- The relationship between the visible brightness of a sampled 8-km pixel and a mean 50-km pixel was investigated on annual and diurnal scales. It was found that there is a distinct regional, seasonal, and diurnal variation in the correlation between the sampled and the areally averaged brightness.
- Computational experiments were performed to obtain statistics on the differences in model derived surface irradiance using sampled instead of averaged satellite visible brightness, or vice versa. It was found that the median RMSE in the model inferred surface insolation in both cases was between 8%–9% of the mean.
- Experiments were conducted to compute the surface irradiance using both satellite sampling methods over targets where ground truth was available. It was demonstrated that it is possible at one time to get better agreement with one type of sampling and at other times better agreement with a different sampling. Evidently, for certain types of cloud conditions, one type of sampling is more compatible with the hourly averaged ground truth than the other. Therefore, before reaching a conclusion on the accuracy of an insolation algorithm, the inherent sampling effects have to be minimized and experiments should be expanded to cover annual time scales, regional spatial scales, different climatic regions, and possibly, the use of variable time averaging of surface observations.

The validation difficulties of satellite derived parameters are becoming recognized. For instance, a major component of the upcoming Tropical Rainfall Measuring Mission (TR) (Simpson et al. 1988) is the

development of sampling strategies for ground and space observations to enable rigorous validation of space estimates of rainfall (Thiele 1987). To address validation of radiation fields, the WMO/ICSU Joint Scientific Committee (JSC) of the WCRP has established a working group on radiative fluxes (WCRP-20 1989), which is overseeing ongoing validation activities. In the present study, selected aspects of validating surface solar irradiance, as derived from satellite observations, have been addressed; the inherent difficulties in the validation process have been illustrated; and possible improvements have been suggested.

Acknowledgments. This work was supported by Grant NAG-5-914 from the National Aeronautics and Space Administration, Earth Science and Applications Division, Climate Research Program, to the University of Maryland. The specialized satellite data were provided by NOAA/NESDIS under the Cooperative Institute for Climate Studies. Thanks are due to the granting agencies to Dr. J. A. Coakley, Jr., for helpful discussions and to Minze V. Chien for technical assistance.

APPENDIX

Mesoscale Variability in Surface Irradiance

A unique mesoscale network (33 ground stations) for observing surface solar irradiance was established during the summer of 1977 for the purpose of verifying satellite derived SW↓ (Tarpley 1979). This information was supplemented with SW↓ data from the NOAA network, as reported in "Monthly Summary Solar Radiation Data," NOAA/Environmental Data and Information Service (EDIS), National Climate Center (NCC), Asheville, N.C., and used to study temporal and spatial variability of SW↓ over central United States. To facilitate comparison with earlier studies (Hay 1983), similar procedures were followed. Latitudinal differences do affect the amount of incident extraterrestrial solar irradiance. Wilson (1978) estimated that during March–September, the extraterrestrial differences due to 3° latitude are within the level of instrument accuracy for North America. However, atmospheric variations have the dominant effect and may mask latitudinal differences. Therefore we did not attempt to detrend the data from latitudinal differences. A line representing a second-order least square fit to the standard deviations of one-day averaged differences as a function of station separation distance were added to Fig. 5 (Case E).

REFERENCES

Aguado, E., 1986: Local-scale variability of daily solar radiation—San Diego County, California. *J. Climate Appl. Meteor.*, **25**, 672–678.

Atwater, M. A., and J. T. Ball, 1978: Intraregional variations of solar radiation in the Eastern United States. *J. Appl. Meteor.*, **17**, 1116–1125.

Baker, D. G., and R. H. Skaggs, 1984: The distance factor in the relationship between solar radiation and sunshine. *J. Climatol.*, **4**, 123–132.

Bonner, W. D., 1966: Case study of thunderstorm activity in relation to the low-level jet. *Mon. Wea. Rev.*, **94**, 167–178.

Briegleb, B. P., P. Minnis, V. Ramanathan and E. Harrison, 1986: Comparison of regional clear-sky albedos inferred from satellite observations and model calculations. *J. Climate Appl. Meteor.*, **25**, 214–226.

Burt, J. E., 1985: *Phys. Geogr.*, **6**, 230–246.

Coakley, J. A., and F. P. Bretherton, 1982: Cloud cover from high-resolution scanner data: detecting and allowing for partially filled fields of view. *J. Geophys. Res.*, **87**, 4917–4932.

Dugas, W. A., and M. L. Heuer, 1985: Relationships between measured and satellite estimated solar irradiance in Texas. *J. Climate Appl. Meteor.*, **8**, 751–757.

ESA SP-248, 1986: Parameterization of land surface characteristics; use of satellite data in climate studies; first results of ISLSCP. *Proc. of an International Conference held in Rome, Italy,* pp. 584.

Frouin, R., and G. Gautier, 1987: Calibration of NOAA-7 AVHRR, GOES-5 and GOES-6 VISSR/VAS solar channels. *Remote Sen. Environ.*, **22**, 73–101.

Gandin, L. S., 1970: The planning of meteorological station networks. WMO-No. 265, TP. 149, pp. 35.

Gautier, C., G. Diak and S. Masse, 1984: An investigation of the effects of spatially averaging satellite brightness measurements on the calculation of insolation. *J. Climate Appl. Meteor.*, **23**, 1380–1386.

Granger, O. E., 1980: Climatology of global solar radiation in California and an interpolation based on orthogonal functions. *Solar Energy*, **24**, 153–168.

Hay, J. E., 1983: An assessment of the mesoscale variability of solar radiation at the earth's surface. *Solar Energy*, **32**, 425–434.

——, and P. W. Suckling, 1979: An assessment of the networks for measuring and modeling solar radiation in British Columbia and adjacent areas of Western Canada. *Can. Geographer*, **XXIII**, 222–238.

Hovis, W. A., J. S. Knoll and G. R. Smith, 1985: Aircraft measurements for calibration of an orbiting space craft sensor. *Appl. Optics*, **24**, 407.

Iqbal, M., 1983: *An Introduction to Solar Radiation.* Academic Press, pp. 390.

Jacobowitz, H., R. J. Tighe and the Nimbus 7 Experiment Team, 1984: The earth radiation budget derived from the Nimbus 7 ERB experiment. *J. Geophys. Res.*, **89**, 4997–5010.

Kaufman, Y. J., T. W. Brakke and E. Eloranta, 1986: Field experiment to measure the radiative characteristics of a hazy atmosphere. *J. Atmos. Sci.*, **43**, 1135–1151.

Kneizys, F., E. Shettle, W. Gallery, J. Chetwynd, L. Abreu, J. Selby, R. Fynn and R. McClatchey, 1980: Atmospheric transmittance–radiance: computer code LOWTRANS. Rep. AFGL-TR-80-67, Air Force Geophysics Laboratory, Hanscom AFB, MA, 127 pp.

Lacis, A. A., and J. E. Hansen, 1974: A parameterization for the absorption of solar radiation in the earth's atmosphere. *J. Atmos. Sci.*, **31**, 118–133.

Latimer, J. R., 1980: Canadian procedures for monitoring solar radiation. *Proc. First Canadian Solar Radiation Data Workshop.*

Matthews, E., 1983: Global vegetation and land use: new high resolution data bases for climate studies. *J. Climate Appl. Meteor.*, **22**, 474–487.

Moyer, W. J., 1968: Climate of Maryland. Climatology of the United States No. 60-18, U.S. Dept. of Commerce, ESSA Environmental Data Service.

Phillips, D. W., and J. Aston, 1980: Canadian solar radiation data. *Environ. Canada*, 1–15.

Pinker, R. T., and J. A. Ewing, 1985: Modeling surface solar radiation: model formulation and validation. *J. Climate Appl. Meteor.*, **24**, 389–401.

——, and I. Laszlo, 1990: Improved prospects for estimating inso-

lation for calculating regional evapotransiration from remotely sensed data. *Agric. and Forest Meteorology,* **52,** 227–251.

Rossow, W. B., F. Mosher, E. Kinsella, A. Arking, M. Desbois, E. Harrison, P. Minnis, E. Ruprecht, G. Seze, C. Simmer and E. Smith, 1985: ISCCP cloud algorithm intercomparison. *J. Climate Appl. Meteor.,* **24,** 877–903.

Schiffer, R. A., and W. B. Rossow, 1985: ISCCP Global Radiance Dataset: a new resource for climate research. *Bull. Amer. Meteor. Soc.,* **66,** 1498–1503.

Schmetz, J., 1989: Towards a surface radiation climatology: retrieval of downward irradiance from satellites. *Atmos. Res.,* **23,** 287–321.

Simpson, J., R. F. Adler and G. North, 1988: A proposed tropical rainfall measuring mission (TRMM) satellite. *Bull. Amer. Meteor. Soc.,* **66,** 278–295.

Stephens, G. L., S. Ackerman and E. Smith, 1984: A shortwave parameterization revised to improve cloud absorption. *J. Atmos. Sci.,* **41,** 687–690.

Tarpley, J. D., 1979: Estimating incident solar radiation at the surface from geostationary satellite data. *J. Appl. Meteor.,* **18,** 1172–1181.

Thiele, O. W., 1987: On requirements for a satellite mission to measure tropical rainfall. NASA Pub. 1183, 49 pp.

Wark, D. O., G. J. Comeyne, Jr., J. S. Knoll and J. H. Lienesch, 1980: Calibration of the GOES/VISSR visible channel and its relevance to radiation balance. IRS 1980, Colorado State University, Fort Collins, CO.

WCP-55, 1983: World Climate Research report of the experts meeting on aerosols and their climate effects. 107 pp.

WCP-92, 1984: Report of the TOGA workshop on sea surface temperature and net surface radiation, 41 pp. [Available from the World Meteorological Organization, Geneva.]

WCP-115, 1986: Report of the workshop on surface radiation budget for climate applications. WMO/TD-No. 109, 144 pp.

WCRP-5, 1988: Concept of the global energy and water cycle experiment. Report of the JSC study group on GEWEX. (WMO/TD-No. 215).

WCRP-10, 1988: Radiation and climate: report of the first session, JSC working group on radiative fluxes, (WMO/TD-No. 235).

WCRP-20, 1989: Radiation and Climate. Report of second session of the WCRP working group on radiative fluxes. (WMO/TD-No. 291).

WCRP-21, 1989: International WOCE scientific Conf. Rep. of the international WOCE scientific Conf., (WMO/TD-No. 295).

Whitlock, C. H., and the SRB Algorithm Validation Team, 1990: Comparison of surface radiation budget satellite algorithms for downwelled shortwave irradiance with Wisconsin FIRE/SRB surface truth data. *Proc., AMS Seventh Conf. on Atmospheric Radiation,* San Fransisco.

Wilson, R. G., 1978: Solar radiation network assessment and design. *Proc., First Canadian Solar Radiation Data Workshop,* 105–117.

——, and D. E. Petzold, 1972: Daily solar radiation differences between stations in Southern Canada: a preliminary analysis. *Climatol. Bull.,* **11,** 15–22.